

Lecture 7. Types of inverse problems, model reduction, model identification.

Part A: Experimental identification of low order model

Jean-Luc Battaglia

Email: jean-luc.battaglia@u-bordeaux.fr

University of Bordeaux
Laboratory I2M, Department TREFLE, UMR 5295
ENSAM, Esplanade des arts et métiers
33405 Talence Cedex, France.

Abstract: The system identification technique is used to formulate a reliable direct model to be used in an inverse heat transfer problem. This approach finds several practical applications in thermal sciences for reasons that will be developed in the text. For clarity, we will restrict our presentation to monovariate linear systems relating the temperature at one point in the system to one heat flux acting on the system. Two approaches are presented in this course. In the first one, the non-parametric method only uses the temperature and heat flux measurement by calculating the cross correlation or power spectral density. The second set of methods relates to the parametric methods that consist in identifying the parameters of a model that expresses the successive time derivatives of the temperature to the heat flux.

Nomenclature

a	Thermal diffusivity $\text{m}^2 \cdot \text{s}^{-1}$	S_{xy}	power spectral density between x and y
C_{xy}	correlation function between x and y	T	temperature, K
C_p	specific heat, $\text{J} \cdot \text{kg}^{-1} \cdot \text{K}^{-1}$	T	time, s
D^ν	derivative of real order ν	$X_s = [x_s, y_s]$	sensor coordinates
e	measurement error	y	temperature measurement, K
h_m	impulse response	V	loss function
h	exchange coefficient, $\text{W} \cdot \text{m}^{-2} \cdot \text{K}^{-1}$	Δt	sampling time
H	transfer function	φ	heat flux density $\text{W} \cdot \text{m}^{-2}$

I^ν	integral of real order ν	ρ	density, kg m ⁻³
k	thermal conductivity, W.m ⁻¹ .K ⁻¹		

Outline

1	Introduction	3
2	The system identification approach.....	6
2.1	The impulse response	6
2.2	The non-parametric approach.....	7
2.2.1	The deconvolution technique	7
2.2.2	The correlation technique.....	9
2.2.3	Spectral technique	10
2.3	The parametric approach.....	10
2.3.1	Principle	10
2.3.2	Output error model	13
2.3.3	Predictive model.....	14
3	Application	15
4	Let's go a little further.....	17
5	Application to heat fluxmeter system identification	20
5.1	Real life context	20
5.2	System identification hardware	22
5.3	Heat transfer model in the fluxmeter.....	25
5.4	Correlation and spectral techniques	26
5.4.1	linear swept-frequency cosine signal	26
5.4.2	PRBS signal.....	27
5.5	Parametric identification - AR models, theoretical background	29
5.6	NI models, theoretical background	30
6	Conclusion.....	31
7	References	31
8	Appendix 1: Matlab codes.....	32
8.1	Correlation method.....	32
8.2	Spectral method.....	33
8.2.1	Parametric estimation.....	33
9	Appendix 2: the non-integer calculus.....	36

1 Introduction

The system identification framework is a well-known domain that has applications in automatic (for control purpose mainly) and in signal processing [1][2]. For several years the heat transfer scientific community found very interesting applications of those methods for the modelling of heat and mass processes that occur in thermal systems [6][7][8]. In this course we present the system identification technique as an efficient tool to formulate a reliable direct model that can be used to solve the corresponding inverse heat transfer problem. In case of a *monovariable system*, as that represented in Figure 1, the inverse procedure will consist in estimating the heat flux acting on the studied system from temperature measurement at one point in the system. Let us highlight now that the methods that will be presented below can be obviously generalized to multivariable systems (several heat flux or heat sources acting on a system equipped with several sensors). As an additional constraint, we will also restrict the presentation of the methods to *linear systems*. It means that the thermal properties of the system will not depend on temperature. However, system identification has been developed for nonlinear systems, but mathematical derivations of such techniques are largely beyond the scope of this course.

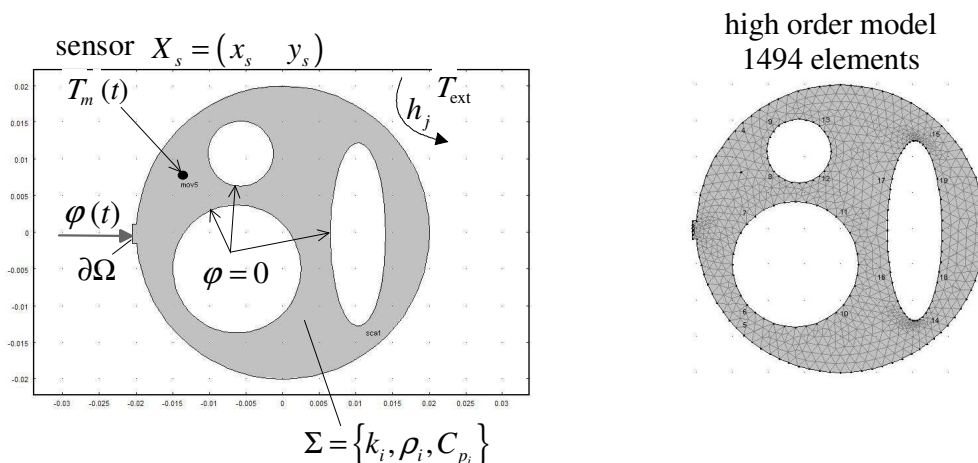


Figure 1: example of a 2D monovariable linear system.

Why are scientists working in the field of heat transfer, and more particularly in measurements inversion, interested with system identification? The first answer relates to model reduction. Indeed, whatever the implemented inverse technique, inversion requires using a direct model in an iterative manner to approach the solution. Statistical methods such as the Bayesian technique require calls upon the direct model many times and computational times could become dramatically long. As an example, let us consider the 2D system represented in Figure 1. The domain Σ is characterized by its thermal properties (thermal conductivity k_i , specific heat per unit volume $C_{p,i}$ and density ρ_i for constitutive material i). A heat flux φ is imposed on the boundary $\partial\Omega$ whereas the remaining part of the outdoor boundary is subjected to convection with the coefficient h_j , the temperature of the surrounding fluid being denoted T_{ext} . Finally, the inner boundaries are insulated. The objective here is to estimate the heat flux density

from temperature measurements in the plate. It is thus assumed that a sensor has been embedded in the plate and the temperature of the sensor is denoted $T_m(t)$. Although this problem is quite simple, only a discrete method (finite elements for example) can be used to solve the heat diffusion equation and associate boundary and initial conditions to simulate the temperature of the sensor. A mesh is thus built (see Figure 1) that leads to calculating the temperature at each node. This discrete model is so-called a *high-order model*, the order referring to the number of degrees of freedom of the mesh. Simulating the output of this model leads to results as those presented in Figure 2.

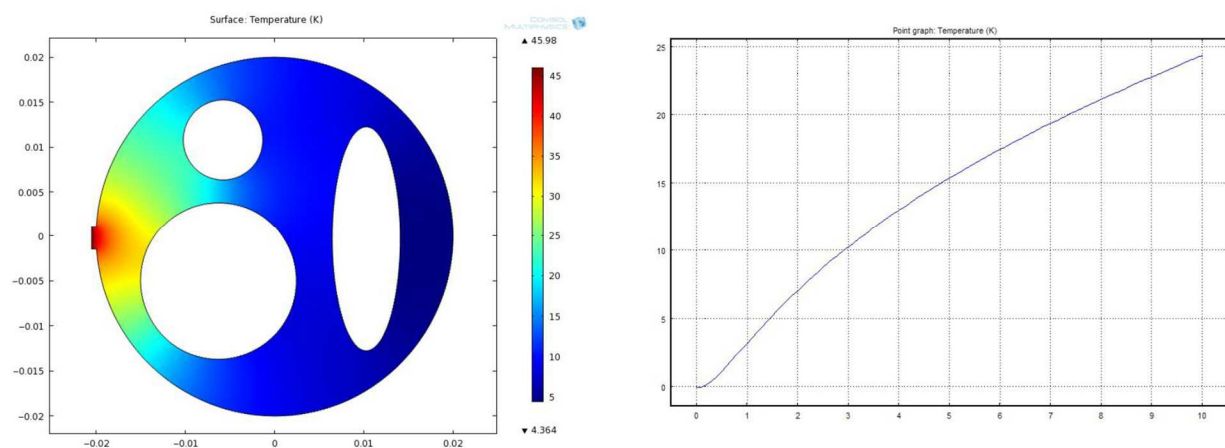


Figure 2: simulation of the temperature field at $t=10$ sec and of the time dependent temperature of the sensor for a step heat flux density.

The reliability of the direct model rests on the accuracy on two sets of data: the thermal properties $\{k_i, C_{p,i}, \rho_i, h_j\}$ and the location $X_s = [x_s, y_s]$ of the sensor. Uncertainties for these data will lead to a very low confidence domain for the estimated heat flux [9].

This system identification approach is described in a schematic way in Figure 3. The goal is to apply a known heat flux $\varphi(t)$ on the system and to measure the signal at the thermal sensor. We must note as a first point that *calibrating the sensor* (the link between the measured signal and the absolute temperature) is not required since the same sensor is used both for identifying the system and the above defined inversion. Once these data given, estimating “a” model \mathbf{M} that relates them becomes possible. However, it must be emphasized that this estimated model has significance on the measurement time-domain only. *Prediction* is therefore a main issue of system identification. Secondly, the measurements are affected by an error (noise) that will have an influence on the identified model. It is generally admitted that the imposed heat flux is generally fully known and that it is errorless. Thus, all the error is reported on the sensor signal. **Obviously, the objective is to use a model \mathbf{M} that is more accurate than that obtained from the FEM with uncertainties on $\{k_i, C_{p,i}, \rho_i, h_j\}$ and $X_s = [x_s, y_s]$.**

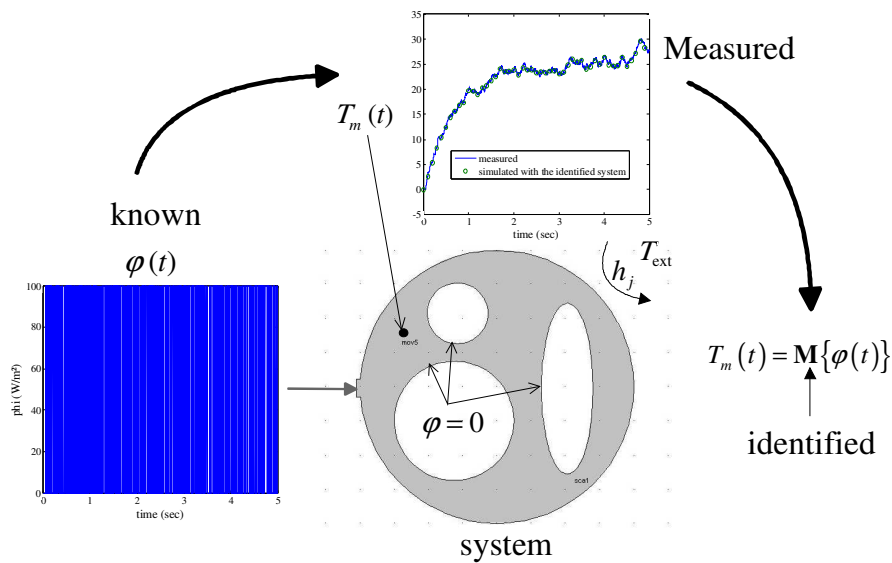


Figure 3: thermal system identification procedure.

Once the thermal system has been identified, it can be used to solve the inverse problem, which is to estimate the heat flux from model \mathbf{M} and from temperature measurement at the sensors. The classical procedure is described in Figure 4.

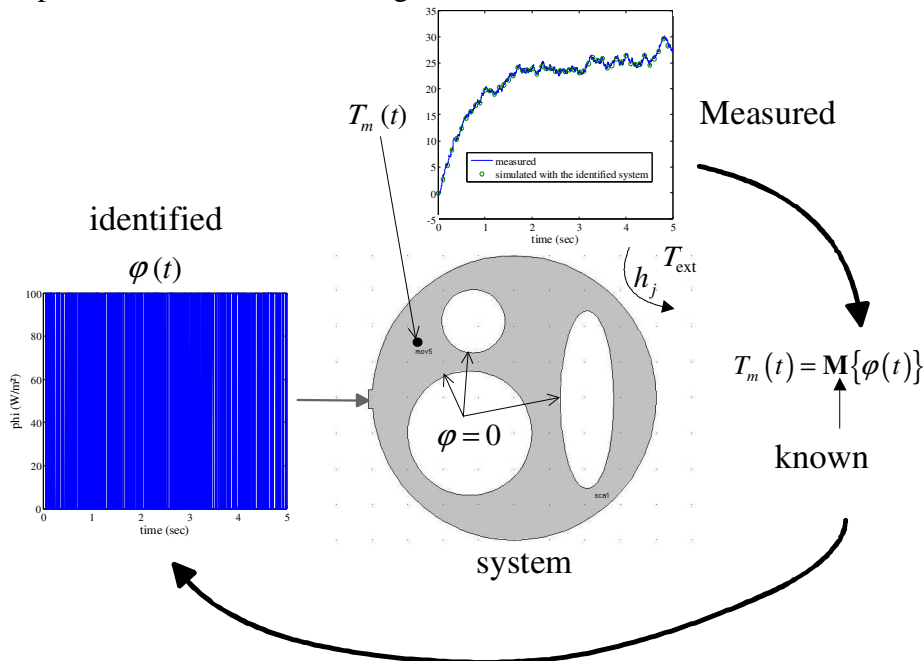


Figure 4: use of the identified system to solve the inverse procedure (estimating the heat flux).

It means that if the identified system model describes the thermal behaviour for the heat flux sequence represented in Figure 3 in a correct manner, it is then expected to retrieve this sequence applying an inverse technique starting from the knowledge of the identified model \mathbf{M} and of the temperature measurement presented in Figure 3. This is what suggests Figure 4.

According to our previous description, it can be thus possible now to draw the main advantages and drawbacks of this approach.

Advantages

- The system identification approach will be first interesting to obtain a reliable and accurate *low order model* that will require less computational time for simulation.
- There is no need to know the thermal properties of the system (thermal conductivity, density, specific heat, heat exchange coefficients, thermal resistances at the interfaces, parameters related to thermal radiation...).
- It is not required to know the sensor location inside the system.
- Calibrating the sensor is not required.
- The identification procedure is fast (this will be viewed later with the description of the different techniques).

Drawbacks

- The model identification must be achieved in the same conditions as those encountered during the inversion (heat exchanges between the surrounding and the system must remain the same for the two configurations).
- The prediction of the identified model rests on strong assumptions (in particular, it is better reaching the stationary behaviour during the system identification process). In general, the identified system is only valid for the time duration of the system identification process.

2 The system identification approach

2.1 The impulse response

The temperature $T_m(t)$ of the sensor is related to the heat flux $\varphi(t)$ thanks to the impulse response $h_m(t)$ under the form of the following convolution product, that is a direct mathematical formulation of the Duhamel's theorem:

$$T_m(t) = T_m(0) + (h_m * \varphi)(t) = \int_0^t h_m(t - \tau) \varphi(\tau) d\tau \quad (1)$$

Let us note here that if temperature $T_m(t)$ is expressed in kelvin, and if heat flux $\varphi(t)$ is in W.m^{-2} , this means that the product $\varphi(t)dt$ is in J.m^{-2} , and consequently the impulse response $h_m(t)$ is in $\text{K.m}^2.\text{J}^{-1}$.

Equation (1) is valid for linear systems with a single transient excitation, with time independent coefficients and zero initial state, where the impulse response fully characterizes the forced thermal behavior. Therefore, any kind of inverse strategy can be based on the direct model expressed in terms of the impulse response of the system. However, as we said in the first section, this impulse response will depend on the following quantities: $\{k_i, C_{p,i}, \rho_i, h_j\}$ and $X_s = [x_s, y_s]$. According to the uncertainty that affects those quantities, the user could imagine directly measuring the impulse response from an experiment. It will consist in replacing the heat flux on the real problem by a *known* photothermal excitation, delivered by a laser for example, and in measuring the temperature of the sensor (case of a pulsed heat flux). However, this approach is not reliable since the impulse response magnitude should be very low to preserve the linear behavior of the system. As an illustration the temperature of the sensor is

calculated in the configuration given above with $\varphi(t) = 10^6 \times \exp(-t^2/\tau^2)$ where $\tau = 1\mu\text{sec}$ is small enough to consider this excitation as a Dirac distribution. The simulation is presented in Figure 5. The maximum amplitude of the response is very low here. The above approximation implies an additional contribution to the measurement error.

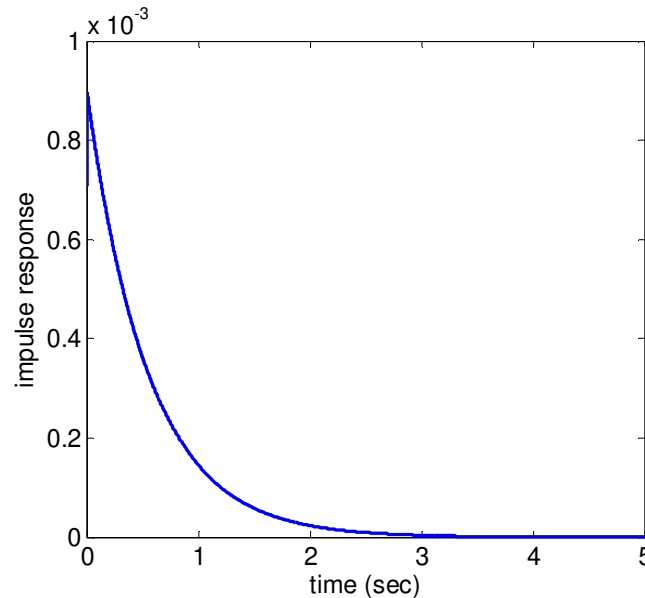


Figure 5: simulation of the impulse response using the FEM.

Another solution could consist in calculating the derivative of the step response shown in Figure 2 (right plot) to retrieve the impulse response. Again, it is not a reliable technique since the derivation will amplify the measurement error and will lead to a very inaccurate impulse response, especially at the short times.

Several powerful techniques have been developed in the system identification and signal processing domains that lead to more accurate identified impulse responses of the system. These techniques are classified in two sets of methods: the non-parametric methods and the parametric ones.

2.2 The non-parametric approach

2.2.1 The deconvolution technique

A very easy technique for the deconvolution of (1) is to consider the discrete form of this relation [2], obtained by the numerical quadrature of the convolution integral, calling $t_f = N \Delta t$ the duration of the experiment, where Δt is the sampling time interval:

$$T_k = T_m(k \Delta t) = T_m(0) + \sum_{i=1}^k \tilde{h}_{m,k-i+1} \tilde{\varphi}_i \Delta t \quad (2)$$

$$\text{where } \begin{cases} \tilde{h}_{m,i} = \frac{1}{\Delta t} \int_{(i-1)\Delta t}^{i\Delta t} h_m(t) dt \approx \frac{1}{2} (h_{m,i-1} + h_{m,i}) \text{ with } h_{m,i} = h_m(i \Delta t) \\ \tilde{\varphi}_i = \frac{1}{\Delta t} \int_{(i-1)\Delta t}^{i\Delta t} \varphi(t) dt \approx \frac{1}{2} (\varphi_{i-1} + \varphi_i) \text{ with } \varphi_i = \varphi_i(i \Delta t) \end{cases} \quad (3)$$

Let us note that, in order to get a forced response, the three functions present in equation (1) should be equal to zero for times t such as $t \leq 0$, and in particular $\varphi(0) = T_m(0) = 0 \Rightarrow h_m(0) = 0$, where the origin of time is the first time where flux φ departs from a zero value. So, the left-hand term of equation (2) is the instantaneous temperature at time $k \Delta t$, while the right terms correspond to average values of the impulse response and of the flux over a time interval. These average values are defined in equation (3) and correspond to the time interval $[(i-1)\Delta t, i \Delta t]$ for $i \geq 1$.

Equation (2a) can be expressed under a vector/matrix form, calling $t_f = N \Delta t$ the duration of the experiment:

$$\begin{bmatrix} T_1 \\ T_2 \\ T_3 \\ \vdots \\ T_N \end{bmatrix} = \begin{bmatrix} T_m(0) \\ T_m(0) \\ T_m(0) \\ \vdots \\ T_m(0) \end{bmatrix} + \Delta t \begin{bmatrix} \tilde{\varphi}_1 & & & & \\ \tilde{\varphi}_2 & \tilde{\varphi}_1 & & & 0 \\ \tilde{\varphi}_3 & \tilde{\varphi}_2 & \tilde{\varphi}_1 & & \\ \vdots & \vdots & \vdots & \ddots & \\ \tilde{\varphi}_N & \tilde{\varphi}_{N-1} & \tilde{\varphi}_{N-2} & \cdots & \tilde{\varphi}_1 \end{bmatrix} \begin{bmatrix} \tilde{h}_{m1} \\ \tilde{h}_{m2} \\ \tilde{h}_{m3} \\ \vdots \\ \tilde{h}_{mN} \end{bmatrix} \quad (4)$$

Assuming an additive measurement error of normal distribution (zero mean and constant standard deviation) for strictly positive times, with a zero error at initial time, the measured temperature is related to the exact one as:

$$y_m(k \Delta t) = T_m(k \Delta t) + e(k \Delta t) - T_m(0) = \Delta t \sum_{i=1}^k \tilde{h}_m(i \Delta t) \tilde{\varphi}((k-i+1) \Delta t) \quad (5)$$

Given that $\lim_{k \rightarrow \infty} h_k = 0$, it is reasonable to truncate the series from $k = Q$ and thus relation (5) becomes:

$$\underbrace{\begin{bmatrix} y_1 \\ y_2 \\ \vdots \\ y_Q \\ \vdots \\ y_N \end{bmatrix}}_{\mathbf{Y}_N} = \Delta t \underbrace{\begin{bmatrix} \tilde{\varphi}_1 & & & & \\ \tilde{\varphi}_2 & \tilde{\varphi}_1 & & & 0 \\ \vdots & \vdots & \ddots & & \\ \tilde{\varphi}_Q & \cdots & \tilde{\varphi}_2 & \tilde{\varphi}_1 & \\ \vdots & & & \vdots & \\ \tilde{\varphi}_N & \cdots & \tilde{\varphi}_{N-Q+1} & \tilde{\varphi}_{N-Q+1} & \end{bmatrix}}_{\Phi_N} \underbrace{\begin{bmatrix} \tilde{h}_{m1} \\ \tilde{h}_{m2} \\ \vdots \\ \tilde{h}_Q \end{bmatrix}}_{\mathbf{H}_Q} + \underbrace{\begin{bmatrix} e_1 \\ e_2 \\ \vdots \\ e_Q \\ \vdots \\ e_N \end{bmatrix}}_{\mathbf{E}_N} \quad (6)$$

Vector \mathbf{H}_Q can thus be estimated in the least square sense, to minimize $(\mathbf{E}_N \mathbf{E}_N^T)$ and one gets:

$$\mathbf{H}_Q = (\Phi_N \Phi_N^T)^{-1} \Phi_N^T \mathbf{Y}_N \quad (7)$$

However, this procedure is quite long according to the values of Q and N and very sensitive to measurement errors.

2.2.2 The correlation technique

A better and faster approach consists in identifying the impulse response $h(t)$, from the cross correlation product of the system response that is the temperature $T_m(t)$ of the sensor and the heat flux $\varphi(t)$ [1]. This method is well suited for non-causal systems, that is for problems where a space coordinate is the independent variable, or to systems where both excitation and response are time periodical. Indeed, let us rewrite relation (5) considering of the measurement errors and assuming that the heat flux is equal to zero for negative times as well as past the current time t :

$$y_m(t) = \int_0^t h_m(t - \tau) \varphi(\tau) d\tau + e(t) = \int_{-\infty}^{+\infty} h_m(t - \tau) \varphi(\tau) d\tau + e(t) \quad (8)$$

where $\varphi(\tau) = 0$ for $\tau \leq 0$ and for $\tau > t$

Now let us multiply the two members of this equality by the lagged heat flux $\varphi(t - \tau)$ and integrates from $t=0$ to infinity. We obtain then:

$$\int_{-\infty}^{+\infty} y_m(t) \varphi(t - \tau) d\tau = \int_{-\infty}^{+\infty} \int_{-\infty}^{+\infty} h_m(t - \tau) \varphi(\tau) \varphi(t - \tau) dt d\tau + \int_{-\infty}^{+\infty} \varphi(t - \tau) e(t) d\tau \quad (9)$$

We see a convolution product between the two functions appears:

$$C_{y_m, \varphi} = \int_{-\infty}^{+\infty} h_m(t - \tau) C_{\varphi, \varphi} d\tau + C_{e, \varphi} \quad (10)$$

If one chose the excitation sequence $\varphi(t)$ as a white noise:

$$C_{\varphi, \varphi}(\tau) = \delta(\tau) \quad (11)$$

And finally, if one admits that the noise measurement is not correlated to the input signal ($C_{e, \varphi} = 0$), one has:

$$C_{y_m, \varphi}(\tau) = h(\tau) \quad (12)$$

It thus appears that the impulse response can be directly deduced from the correlation function between the temperature of the sensor and the heat flux. In practice the correlations functions are calculated using the Fast Fourier Transform of the signals (see next section and Matlab code in Appendix 1).

The interest of the correlation analysis is to make the identification of the physical system under less energy constraints for the magnitude of the heat flux. Indeed, in opposition to pulse analysis, the energy does not have to be deposited in an intense way during a very short time (closest to a Dirac distribution). An interesting feature of such an approach is that the linearity and stationarity assumptions are clearly satisfied, and that the confidence domain of the estimated impulse response is the same all over all the explored frequency range.

2.2.3 Spectral technique

The correlation technique is very sensitive to the magnitude of the measurement noise and practically using the power spectral density instead of the correlation functions [4] is more interesting:

$$\text{FFT}[C_{y_m\varphi}(\tau)] = \text{FFT}\left[\int_0^\infty h_m(t-\tau) C_{\varphi\varphi}(\tau) d\tau\right] = Y_m(f) \Phi(f) = S_{y_m\varphi}(f) \quad (13)$$

and

$$\text{FFT}[C_{\varphi\varphi}(\tau)] = \text{FFT}\left[\int_0^\infty \varphi(t-\tau) \varphi(\tau) d\tau\right] = \Phi(f)^2 = S_{\varphi\varphi}(f) \quad (14)$$

$Y_m(f)$ and $\Phi(f)$ are the Fourier transforms of the temperature and of the heat flux respectively. In a similar way, $S_{\varphi\varphi}(f)$ and $S_{y_m\varphi}(f)$ are the auto and cross PSD (Power Spectral Density). Then, applying the Fourier transform on relation (10) yields immediately:

$$S_{y_m\varphi}(f) = H(f) S_{\varphi\varphi}(f) + S_{\varphi e}(f) \quad (15)$$

Finally, assuming that the noise measurement is not correlated with the heat flux ($S_{\varphi e}(f) = 0$), the expression of the transfer function is:

$$H(f) = \frac{S_{y_m\varphi}(f)}{S_{\varphi\varphi}(f)} \quad (16)$$

Since the duration of the experiment is set to a fixed value τ , the real input signal is:

$$\varphi_{\Pi}(t) = \varphi(t) \Pi_{\tau}(t) \quad (17)$$

In this relation, $\Pi_{\tau}(t) = 1$ when $0 \leq t \leq \tau$ and 0 elsewhere. Then applying the Fourier transform for the heat flux leads to:

$$\Phi_{\Pi}(f) = \Phi(f) * \left(\tau \frac{\sin(\pi \tau f)}{\pi \tau f} \right) \quad (18)$$

It appears that the Fourier transform of the heat flux is convoluted by the cardinal Sine function. Usually, the heat flux is pre-windowed by a specific function $g_{\tau}(t)$ that decreases the influence of the function $\Pi_{\tau}(t)$ as:

$$\varphi_{\Pi}(t) = \varphi(t) g_{\tau}(t) \quad (19)$$

For example, the Hanning window [3][4] is often used. It is defined as:

$$g_{\tau}(t) = 0.5 \left(1 - \cos\left(\frac{2\pi t}{\tau}\right) \right) \quad (20)$$

An improved estimation of $S_{y_m\varphi}(f)$ and $S_{\varphi\varphi}(f)$ has also been proposed by Welch [5]. The method consists in dividing the time series data into possible overlapping segments, computing the auto and cross power spectral densities and averaging the estimates.

2.3 The parametric approach

2.3.1 Principle

The principles of the system identification method are presented by Ljung [1]. Assuming a linear and stationary system, that means that the thermal properties of the system do not vary with temperature and time, the method consists in identifying the parameters involved in a linear relation between the heat flux $\varphi(t)$ and the temperature $T_m(t)$ of the sensor, from

measurements of these two quantities. Without any kind of physical consideration of the heat transfer process, it is assumed a general relationship of the following form is assumed:

$$T_m(t) + \alpha_1 \frac{dT_m(t)}{dt} + \alpha_2 \frac{d^2T_m(t)}{dt^2} + \dots = \beta_0 \varphi(t) + \beta_1 \frac{d\varphi(t)}{dt} + \beta_2 \frac{d^2\varphi(t)}{dt^2} + \dots \quad (21)$$

This kind of model is consistent with the behaviour of the dynamical systems, and it is also the case for thermal systems since the heat diffusion equation rests on the first order derivative of the temperature for all the points of the system. It is thus reasonable to admit that the temperature at time t must depend on the heat flux value at time t and at previous times. On the other hand, since temperature at times before t depends on the heat flux at previous times also, it is not surprising that they appear in the model.

Let us illustrate it on a simple configuration by considering the one-dimensional heat transfer in a wall (thermal conductivity k and thermal diffusivity a) subjected to the heat flux $\varphi(t)$ at $x = 0$ and insulated on the other face at $x = e$. The model is thus:

$$\frac{\partial T(x,t)}{\partial t} = a \frac{\partial^2 T(x,t)}{\partial x^2}, 0 < x < e, t > 0 \quad (22)$$

The boundary conditions are:

$$-k \frac{\partial T(x,t)}{\partial x} = \varphi(t), x = 0, t > 0 \quad (23)$$

$$\frac{\partial T(x,t)}{\partial x} = 0, x = e, t > 0 \quad (24)$$

And the initial condition is chosen as:

$$T(x, t) = 0, 0 \leq x \leq e, t = 0 \quad (25)$$

Let us examine the temperature at $x = e$ and we note $T_m(t) = T(x = e, t)$. The Laplace transform $L\{ \}$ is used to solve the previous problem:

$$L\{T_m(t)\} = \theta_m(s) = \frac{1}{k \beta \sinh(\beta e)} L\{\varphi(t)\} = \frac{1}{k \beta \sinh(\beta e)} \Phi(s) \quad (26)$$

Where: $\beta = \sqrt{s/a}$. The hyperbolic sine function can be expressed as the following series:

$$\sinh(z) = \sum_{n=0}^{\infty} \frac{z^{2n+1}}{(2n+1)!}, \forall z \geq 0 \quad (27)$$

Replacing this expression in relation (26) yields:

$$\theta_m(s) = \frac{1}{k \beta \sum_{n=0}^{\infty} \frac{(\beta e)^{2n+1}}{(2n+1)!}} \Phi(s) = \frac{1}{k \sum_{n=0}^{\infty} \frac{e^{2n+1} s^{n+1}}{a^{n+1} (2n+1)!}} \Phi(s) \quad (28)$$

That can be also written as:

$$\sum_{n=0}^{\infty} \alpha_n s^{n+1} \theta_m(s) = \Phi(s) \quad (29)$$

With: $\alpha_n = k \frac{e^{2n+1}}{a^{n+1} (2n+1)!}$.

At this stage we must remind us of an important property related to the Laplace transform of the derivative of a function:

$$L\left(\frac{d^n f(t)}{dt^n}\right) = s^n F(s) - \sum_{k=0}^{n-1} s^{n-k-1} \frac{d^k f(0)}{dt^k} \quad (30)$$

Taking into account the initial condition (25), relation (29) becomes :

$$\sum_{n=0}^{\infty} \alpha_n \frac{d^{n+1} T_m(t)}{dt} = \varphi(t) \quad (31)$$

It is therefore demonstrated that the heat transfer model expressing the temperature at $x = e$ according to the heat flux $\varphi(t)$ imposed at $x = 0$ can be put on the form of the relation (21). In fact the series in (31) can be significantly truncated and we will thus obtain a *low order model*.

The discrete form of the derivatives gives rise to an equivalent form of relation (21) and temperature at time $k \Delta t$ depends on the heat flux and the temperature at previous times as:

$$T_m(k) = b_0 \varphi(k) + b_1 \varphi(k-1) + b_2 \varphi(k-2) + \dots - a_1 T_m(k-1) - a_2 T_m(k-2) - \dots \quad (32)$$

Let us note that replacing the temperature at previous times with the measurement in relation (32) leads to the predictive model as:

$$\hat{T}_m(k) = b_0 \varphi(k) + b_1 \varphi(k-1) + b_2 \varphi(k-2) + \dots - a_1 y_m(k-1) - a_2 y_m(k-2) - \dots \quad (33)$$

Relation (32) is called the output error model whereas relation (33) is called the predictive model. Identification of parameters (a_i, b_j) will significantly differ according to the choice of the model as represented in Figure 6.

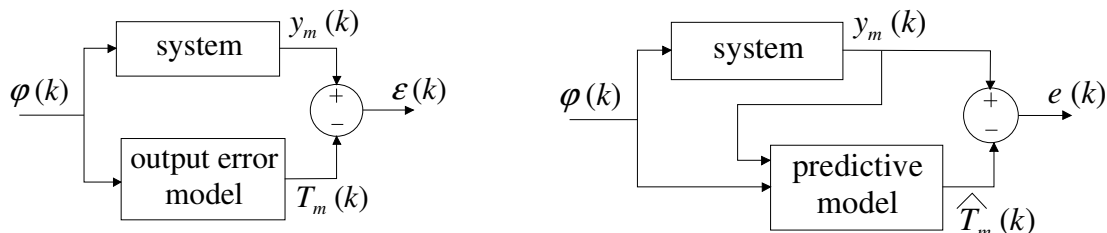


Figure 6: parameter identification according to the model representation (output error or predictive).

In case of the output error model configuration, the sensitivity functions $S(a_i) = dT_m(t)/da_i$ and $S(b_j) = dT_m(t)/db_j$ depend on the parameters a_i and b_j . It means that the minimization of $\rho(N) = \sum_{k=0}^N \varepsilon(k)^2$ requires a non-linear minimization algorithm. On the other side, the sensitivity functions do not depend anymore on the parameters when minimizing the quantity

$r(N) = \sum_{k=0}^N e(k)^2$. It means that estimation of the parameters in case of the predictive model is implemented by a linear minimization algorithm.

2.3.2 Output error model

Let us assume that the number of parameters is n for a_i and $(n+1)$ for b_j . The sensitivity functions of the temperature at time $k \Delta t$ with respect to a_i and b_j are:

$$S_{a_i}(k) = \frac{\partial T_m(k)}{\partial a_i}, i = 1, \dots, n \quad (34)$$

$$S_{b_i}(k) = \frac{\partial T_m(k)}{\partial b_i}, i = 0, \dots, n \quad (35)$$

According to relation (32), it is obtained:

$$S_{a_i}(k) + a_1 S_{a_i}(k-1) + \dots + a_n S_{a_i}(k-n) = -T_m(k-i), i = 1, \dots, n \quad (36)$$

With: $S_{a_i}(0) = S_{a_i}(1) = \dots = S_{a_i}(n-1) = 0$

And:

$$b_0 S_{b_i}(k) + b_1 S_{b_i}(k-1) + \dots + b_n S_{b_i}(k-n) = \varphi(k-i), i = 0, \dots, n \quad (37)$$

With: $S_{b_i}(0) = S_{b_i}(1) = \dots = S_{b_i}(n-1) = 0$.

Therefore, the output error at time $k \Delta t$ is:

$$\varepsilon(k) = y_m(k) - T_m(k) = \sum_{i=1}^n S_{a_i}(k) \Delta a_i + \sum_{i=0}^n S_{b_i}(k) \Delta b_i \quad (38)$$

Let us imagine that measurements are collected from $n \Delta t$ up to $N \Delta t$. A matrix representation of (38) of the following form is thus obtained:

$$\mathbf{E} = \begin{bmatrix} \varepsilon(n) \\ \varepsilon(n+1) \\ \vdots \\ \varepsilon(N) \end{bmatrix} = \mathbf{S} \begin{bmatrix} \Delta a_1 \\ \vdots \\ \Delta a_n \\ \Delta b_0 \\ \vdots \\ \Delta b_n \end{bmatrix} = \mathbf{S} \Delta \Theta \quad (39)$$

Where:

$$\mathbf{S} = \begin{bmatrix} S_{a_1}(n) & \dots & S_{a_n}(n) & S_{b_0}(n) & \dots & S_{b_n}(n) \\ \vdots & & \vdots & \vdots & & \vdots \\ S_{a_1}(N) & \dots & S_{a_n}(N) & S_{b_0}(N) & \dots & S_{b_n}(N) \end{bmatrix} \quad (40)$$

Solving equation (39) in the least square sense leads to:

$$\Delta \Theta = (\mathbf{S}^T \mathbf{S})^{-1} \mathbf{S}^T \mathbf{E} \quad (41)$$

It is thus possible to obtain the optimal value of Θ using an iterative scheme as:

$$\Theta_v = \Theta_{v-1} + \Delta \Theta_{v-1} \quad (42)$$

2.3.3 Predictive model

Relation (33) can be put under the form:

$$y_m(k) = \mathbf{H}(k) \Theta + e(k) \quad (43)$$

Where $\Theta^T = [a_1 \ \dots \ a_n \ b_0 \ \dots \ b_n]$ and \mathbf{H} is the regression vector defined as:

$$\mathbf{H}(k) = [-y_m(k-1) \ \dots \ -y_m(k-n) \ \varphi(k) \ \dots \ \varphi(k-n)] \quad (44)$$

Let us imagine that measurements are collected from $n \Delta t$ up to $N \Delta t$. Therefore, relation (43) leads to:

$$\mathbf{Y}_N = \Psi_N \Theta + \mathbf{E}_N \quad (45)$$

Where:

$$\mathbf{Y}_N^T = [y_m(n) \ \dots \ y_m(N+n)], \Psi_N^T = [\mathbf{H}(n) \ \dots \ \mathbf{H}(N+n)] \text{ and } \mathbf{E}_N^T = [e(n) \ \dots \ e(N+n)].$$

An estimation of Θ in the linear least square sense is obtained as:

$$\hat{\Theta} = (\Psi_N \Psi_N^T)^{-1} \Psi_N^T \mathbf{Y}_N \quad (46)$$

Despite of the rapidity of the method, it must be noted that the estimation is biased. Indeed, let us replace the expression of the identified parameters, relation (46), in the model, relation (43). It is found:

$$\hat{\Theta} = \Theta + (\Psi_N \Psi_N^T)^{-1} \Psi_N^T \mathbf{E}_N \quad (47)$$

It is demonstrated in the literature that:

$$E\{\hat{\Theta}\} = \Theta + (E\{\mathbf{H}(k) \mathbf{H}(k)^T\})^{-1} E\{\mathbf{H}(k)^T e(k)\} \quad (48)$$

It thus appears that if $e(k)$ is correlated with $\mathbf{H}(k)$ or if $E\{e(k)\}$ is not zero, the estimation is biased and $E\{\hat{\Theta}\} \neq \Theta$.

To accelerate the identification of Θ , a recursive scheme can be used. The vector of parameters at instant t is estimated from parameters estimated previously at instant $(t-1)$ according to:

$$\hat{\Theta}(k) = \hat{\Theta}(k-1) + \mathbf{L}(k)[y_m(k) - \mathbf{H}(k)\hat{\Theta}(k-1)] \quad (49)$$

With:

$$\mathbf{L}(k) = \frac{\mathbf{P}(k-1) \mathbf{H}(k)^T}{\lambda(k) + \mathbf{H}(k) \mathbf{P}(k-1) \mathbf{H}(k)^T}$$

And:

$$\mathbf{P}(k) = \mathbf{P}(k-1) - \frac{\mathbf{P}(k-1) \mathbf{H}(k)^T \mathbf{H}(k) \mathbf{P}(k-1)}{\lambda(k) + \mathbf{H}(k) \mathbf{P}(k-1) \mathbf{H}(k)^T}$$

where the initial values are: $\hat{\Theta}(0) = \mathbf{0}_D$ and $\mathbf{P}(0) = 10^6 \mathbf{I}_D$, with $\mathbf{0}_D$ and \mathbf{I}_D are zeros vector and unity matrix respectively with dimension $D = 2N$.

Remark: unbiased approaches are proposed in the literature that consist in whitening the sequence $e(k)$ in relation to (43). This is the instrumental variables method, and methods based on the change of the model structure (auto regressive with exogeneous input model = ARX, auto regressive with adjusted mean and exogeneous input model for example).

3 Application

Let us consider the heat transfer problem presented above and let us generate a heat flux sequence under the form of the pseudo random binary sequence represented in Figure 7. Such a choice for the excitation sequence makes the identification quite easy in practice. This sequence is also very close to a white noise in terms of the power spectral density as represented in Figure 8.

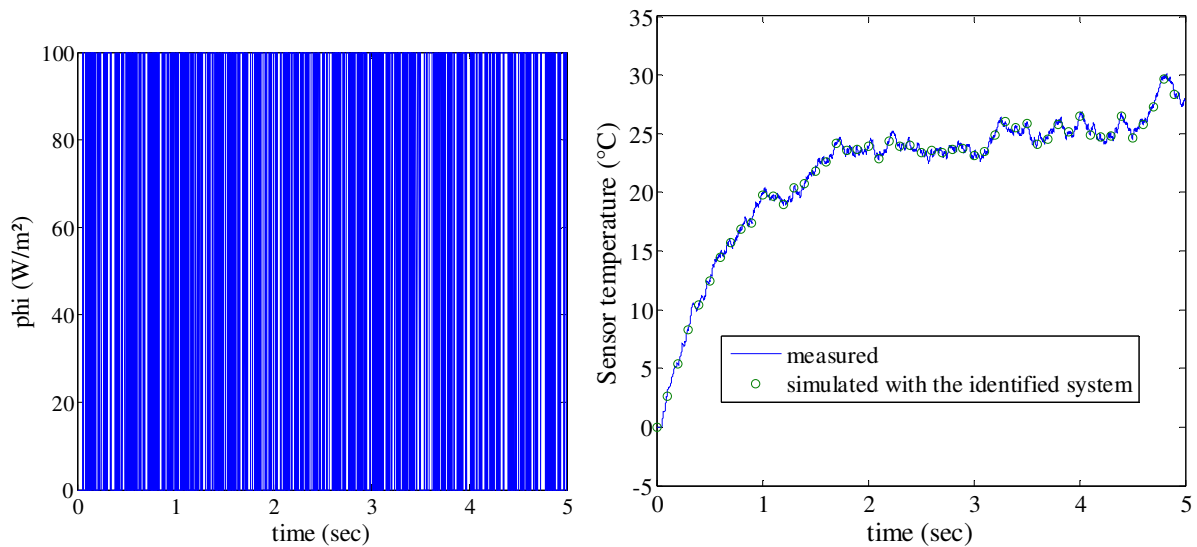


Figure 7: image on the left – heat flux generated on the form of a PRBS; image on the right – measured temperature of the sensor and comparison with the simulation of the identified system.

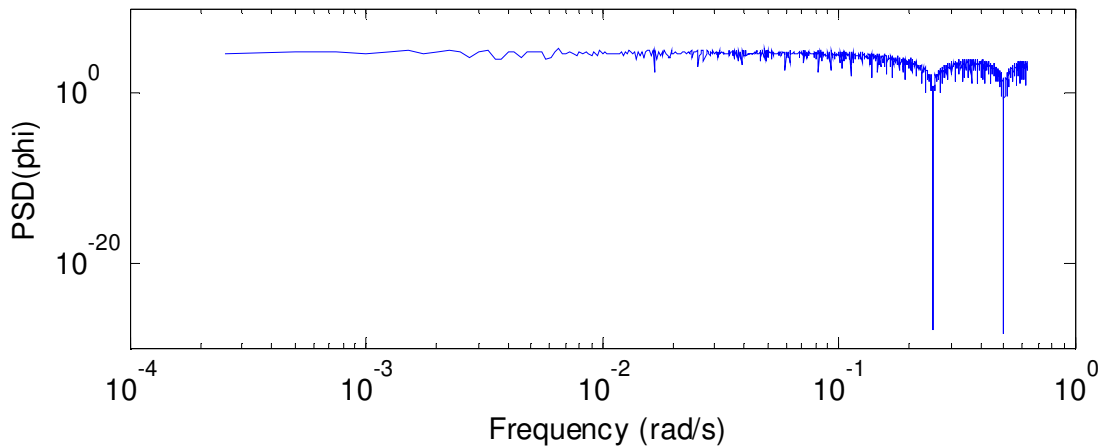


Figure 8: power spectral density of the heat flux generated as a PRBS.

Using the correlation method described previously, the impulse response represented in Figure 9 is obtained. This figure shows that the impulse response reconstructed using the correlation technique is very sensitive to noise the measurement noise.

In a second stage, we used the parametric approach in order to find the model on the form of the relation (33) that best fits the experimental measurements (Figure 7). The choice of $\Lambda = [na, nb]$ (na is the number of parameters a_i and nb is the number of parameters b_i) is made by collecting in a matrix all the values of Λ to be investigated and looking for the value of the Aikake [1] criterion defined by

$$\Psi = \frac{1+n/N}{1-n/N} V, n = na + nb + 1 \quad (50)$$

where n is the total number of estimated parameters and V is the loss function defined by

$$V = \sum_{k=1}^N e_k^2 \quad (51)$$

Standard errors of the estimates are calculated from the covariance matrix of $\hat{\Theta}$. If the assumptions of additive, zeros mean, constant variance σ^2 and uncorrelated errors are verified, the covariance matrix is expressed as

$$\text{cov}(\hat{\Theta}) = (\mathbf{H}^T \mathbf{H})^{-1} \sigma^2 \quad (52)$$

An estimate of the variance σ^2 , denoted s^2 , is:

$$s^2 = \frac{1}{N-n} \mathbf{E}^T \mathbf{E} \quad (53)$$

It is found the optimal set of parameters (a_i, b_i) as:

Parameter	value	Standard deviation	Parameter	value	Standard deviation

a_0	1	0	a_5	0.0166	0.0054
a_1	0.2823	0.01364	b_0	0.0007006	5.348e-006
a_2	0.2539	0.01368	b_1	0.0006788	1.19e-005
a_3	0.2715	0.01375	b_2	0.0004693	1.404e-005
a_4	0.2047	0.01427	b_3	0.0002561	1.365e-005

The loss function is $V=0.000123859$.

Simulating the response with the heat flux sequence brings a very good agreement with measured data as represented in Figure 7. Therefore, the impulse response of the identified system is reported in Figure 9. A very nice agreement with that calculated from the FEM is found. The main difference occurs for short times.

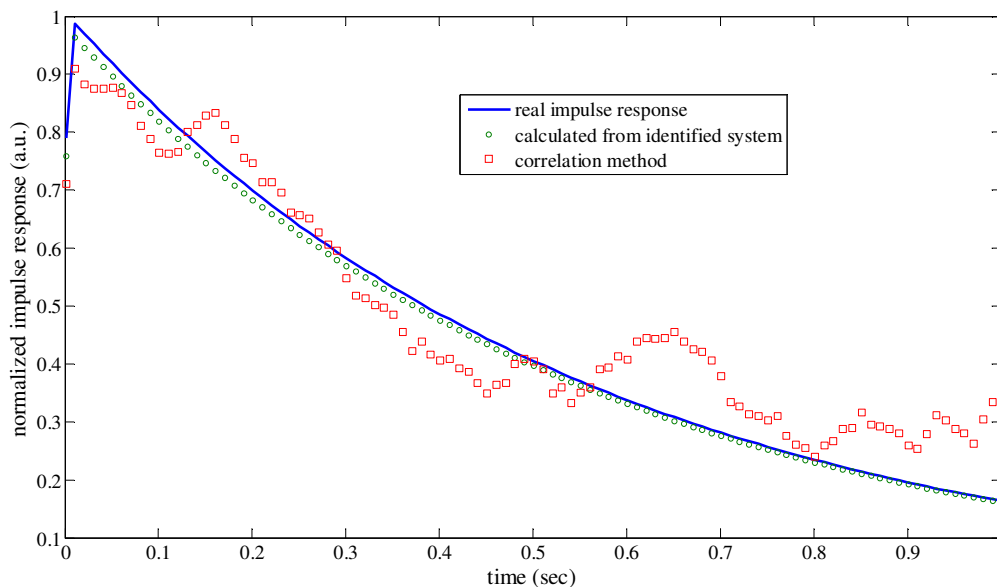


Figure 9: real impulse response and impulse response found using the correlation method and the parametric method.

4 Let's go a little further

Let us consider again the configuration of heat transfer in a wall studied before but let us focus now on the temperature $T_m(t)$ at $x=0$ where the heat flux is applied. Using the Laplace transform to solve the heat diffusion equation with associated boundary and initial conditions (relations (22) to (25)), it is obtained [10]:

$$L\{T_m(t)\} = \theta_m(s) = \frac{\cosh(\beta e)}{k\beta \sinh(\beta e)} L\{\varphi(t)\} = \frac{\cosh(\beta e)}{k\beta \sinh(\beta e)} \Phi(s) \quad (54)$$

Where: $\beta = \sqrt{s/a}$. The hyperbolic functions can be expressed as the following series:

$$\cosh(z) = \sum_{n=0}^{\infty} \frac{z^{2n}}{(2n)!} \text{ and } \sinh(z) = \sum_{n=0}^{\infty} \frac{z^{2n+1}}{(2n+1)!}, \forall z \quad (55)$$

Replacing these expressions in relation (54) it is found:

$$\theta_m(s) = \frac{\sum_{n=0}^{\infty} \frac{(\beta e)^{2n}}{(2n)!}}{k\beta \sum_{n=0}^{\infty} \frac{(\beta e)^{2n+1}}{(2n+1)!}} \Phi(s) = \frac{\sum_{n=0}^{\infty} \frac{e^{2n} s^n}{a^n (2n)!}}{k \sum_{n=0}^{\infty} \frac{e^{2n+1} s^{n+1}}{a^{n+1} (2n+1)!}} \Phi(s) \quad (56)$$

That can be also written as:

$$\sum_{n=0}^{\infty} \alpha_n s^{n+1} \theta_m(s) = \sum_{n=0}^{\infty} \beta_n s^n \Phi(s) \quad (57)$$

With: $\alpha_n = k \frac{e^{2n+1}}{a^{n+1} (2n+1)!}$ and $\beta_n = \frac{e^{2n}}{a^n (2n)!}$.

Taking the initial condition (25) into account and using the property (30) relation (52) becomes equivalent to:

$$\sum_{n=0}^{\infty} \alpha_n \frac{d^{n+1} T_m(t)}{dt} = \sum_{n=0}^{\infty} \beta_n \frac{d^n \varphi(t)}{dt} \quad (58)$$

It is therefore demonstrated that the heat transfer model expressing the temperature at $x=0$ as a function of the heat flux $\varphi(t)$ imposed at $x=0$ can be put on the form of the relation (21). However, if one tries to fit experimental data by simulating the model in relation (53) it appears necessary to keep a very important number of terms in the series to reproduce accurately the transient response at the short times. In that case relation (53) cannot be viewed as a lower order model and moreover, the identification of parameters $\{\alpha_n, \beta_n\}$ becomes inaccurate when n becomes large. It means that the model structure on the form of relation (21) is not optimal for all the possible configurations.

Let's try first to understand such an observation and let's try to find a better low order model structure that would approach the searched optimality.

The reason why model (21) is not pertinent for describing the behaviour at the short times is given in the expression of the asymptotic behaviour at the short times. Indeed, relation (54) shows that:

$$\lim_{s \rightarrow \infty} \frac{\cosh(e\sqrt{s}/\sqrt{a})}{ke\sqrt{s}/\sqrt{a}\sinh(e\sqrt{s}/\sqrt{a})} = \frac{1}{k/\sqrt{a}\sqrt{s}} \quad (59)$$

On the other hand, taking the same limit for relation (56) give:

$$\lim_{s \rightarrow \infty} \frac{\sum_{n=0}^{\infty} \beta_n s^n}{\sum_{n=0}^{\infty} \alpha_n s^{n+1}} = \frac{\beta_n s^n}{\alpha_n s^{n+1}} = \frac{2n+1}{ek/a} \frac{1}{s} \quad (60)$$

It is thus obvious that relation (54) and equivalent relation (56) do not have the same asymptotic behaviour at the short times. In other words the exact asymptotic behaviour, described by relation (59), is that of the semi-infinite medium ($\propto 1/\sqrt{s}$) whereas that of the equivalent model

describes a capacitance effect ($\propto 1/s$). It means that the contribution of an infinite number of derivatives is theoretically required to approach the semi-infinite behaviour of the system.

Is it then possible to find a better low order model that will respect the asymptotic behaviour at the short times? The answer is fortunately yes thanks to the works of Liouville in the 19th century [11][12]. He demonstrated that the property:

$$L\left(\frac{d^{\nu}f(t)}{dt^{\nu}}\right) = s^{\nu}F(s) - \sum_{k=0}^{n-1} s^{n-k-1} \frac{d^k f(0)}{dt^k} \quad (61)$$

remains exact even if ν is real and more generally complex. $D^{\nu}\{f(t)\} = d^{\nu}f(t)/dt^{\nu}$ is called the derivative of real order ν (often called the non-integer derivative in order to discriminate from the classical derivative) and is defined as [13][14][15]:

$$D^{\nu}\{f(t)\} = D^n\{I^{n-\nu}\{f(t)\}\}, n \in \mathbb{N}, \text{Re}(\nu) > 0, n - 1 \leq \text{Re}(\nu) < n \quad (62)$$

where the integral or real order ν is defined in the Liouville sense as:

$$I^{\nu}\{f(t)\} = \frac{1}{\Gamma(\nu)} \int_0^t (t-u)^{\nu-1} f(u) du, \text{Re } \nu > 0 \quad (63)$$

With:

$$\Gamma(\nu) = \int_0^{\infty} u^{\nu-1} \exp(-u) du \quad (64)$$

Regarding to relation (59), it is now clear that:

$$L^{-1}\left\{\frac{1}{k/\sqrt{a}} \frac{1}{\sqrt{s}} \Phi(s)\right\} = \frac{1}{k/\sqrt{a}} I^{1/2}\{\varphi(t)\} \quad (65)$$

Finally, we can say that, instead of relation (21), an optimal structure of a low order model for heat transfer problem by diffusion must be of the following form:

$$\sum_{n=0}^{\infty} \alpha_n D^{n/2}\{T_m(t)\} = \sum_{n=0}^{\infty} \beta_n D^{n/2}\{\varphi(t)\} \quad (66)$$

Let us demonstrate it on the 1D heat diffusion problem in a wall when $T_m(t)$ is the temperature at $x=0$. We saw that we could not find an equivalence of the exact solution (54) under the form of relation (53). In fact, it comes from the manner we have replaced the hyperbolic functions with their series. Let us use the expression of the hyperbolic functions in terms of the exponential:

$$\cosh(z) = \frac{e^z + e^{-z}}{2} = \frac{e^{-z}(1+e^{2z})}{2} \quad (67)$$

And:

$$\sinh(z) = \frac{e^z - e^{-z}}{2} = \frac{e^{-z}(-1+e^{2z})}{2} \quad (68)$$

Replacing these expressions in relation (54) gives:

$$\theta_m(s) = \frac{e^{2\beta e}}{k\beta(e^{2\beta e}-1)} \Phi(s) \quad (69)$$

The series expansion of the exponential is:

$$e^z = \sum_{n=0}^{\infty} \frac{z^n}{n!}, \forall z \quad (70)$$

Replacing this decomposition in relation (69) lead to:

$$\theta_m(s) = \frac{\sum_{n=0}^{\infty} \beta'_n s^{n/2}}{\sum_{n=0}^{\infty} \alpha'_n s^{(n+1)/2}} \Phi(s) \quad (71)$$

With:

$$\alpha'_n = \frac{ke^{n-1}}{a^{(n-1)/2}n!} \text{ and } \beta'_n = \frac{e^{n-1}}{a^{(n-2)/2}n!} \quad (72)$$

It is now possible to find a consistent equivalent expression of the exact solution whose asymptotic behaviour at the short times ($z \rightarrow \infty$) is exactly the relation (59). Going back to time, relation (71) becomes [16][17]:

$$\sum_{n=0}^{\infty} \alpha'_n D^{(n+1)/2} \{T_m(t)\} = \sum_{n=0}^{\infty} \beta'_n D^{n/2} \{\varphi(t)\} \quad (73)$$

Let us insist on the fact that relations (53) and (73) are both exact. The difference lies in the fact that an infinite number of terms are required in relation (53) to describe the response at the short times, when the system behaves as a semi-infinite medium, whereas only a single one is necessary using relation (73).

The Matlab code for the implementation of the technique is given in Appendix 1. It uses the recursive approach presented previously for the classical (with integer derivatives) parametric technique.

5 Application to heat fluxmeter system identification

5.1 Real life context

In high enthalpy plasma flows for aerospace applications but also in high power pulsed laser physics as well as in laser surface hardening monitoring, very high heat fluxes of the order of several MW.m⁻² must be measured (see Figure 10). Only transient measurement techniques have been developed so far. Recently, fast transient heat flux measurements have been conducted using a novel calibration approach. In principle, these sensors can stay a very short time, of the order of milliseconds, in the harsh environment in order not to reach their melting temperature. The transient response of the sensor recorded during this short time is used to estimate the heat flux.

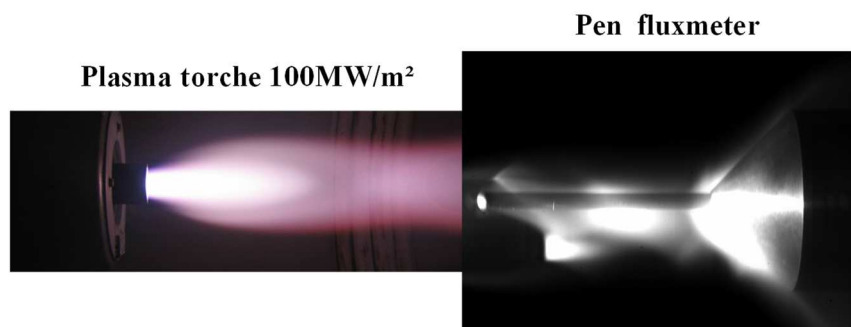


Figure 10: heat flux measurement in a plasma flow using a fluxmeter.

One basic principle of such a heat flux sensor is to measure the temperature, usually with a thermocouple embedded inside an appropriate material which is part of the sensor, and to estimate the heat flux from inverse heat conduction calculation. Consequently, highest reliability in terms of measurement accuracy and local resolution within the sensor is reached when the distance between the temperature measurement and the heated surface is small (see Figure 11). Solving the inverse heat conduction problem requires a model, so-called direct model (DM) of the heat transfer from the heated surface of the sensor to the location of the thermocouple inside the sensor. Models presented in the literature generally assume that the sensor behaves like a semi-infinite wall.

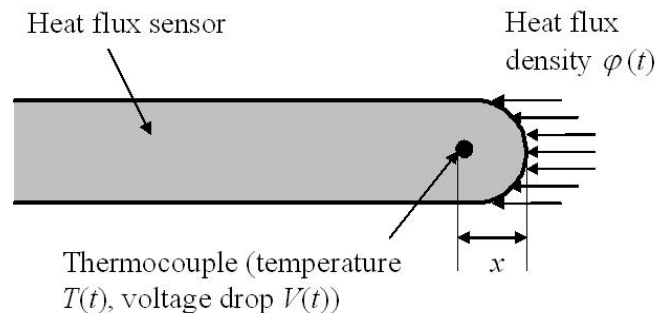


Figure 11: fluxmeter description

Considering a particular sensor and linear heat transfer, i.e., constant material properties for the measurement time, the Duhamel's theorem makes sure that the DM can be viewed as the impulse response. This is the transient temperature of the thermocouple due to a heat flux on the form of a Dirac distribution. If the sensor behaves as a semi-infinite wall, the impulse response is analytically expressed according to the thermal properties of the medium as well as to the location of the thermocouple inside the sensor. However, in real configuration, the heat flux sensors integrate several types of materials arranged in a complicated way. The knowledge of their thermophysical properties as well as the thermal contact resistances at the interfaces must be known if one wants to use the finite element method to solve a detailed DM. Furthermore, it appears that the thermocouple rise time can be larger than the sampling time interval during the acquisition process. This means that the thermocouple junction is not at a uniform temperature for each acquisition time. In other words, a temperature gradient exists in the junction, and one must also consider heat diffusion inside the junction. Obviously, applying the electrothermal conversion between the voltage drop and the temperature of the thermocouple is not allowed here since it rests on the assumption of a uniform temperature of the junction.

To overcome these problems, the basic idea rests on the system identification of the heat flux sensor. It consists in calibrating the sensor by applying a measurable transient heat flux in the time domain of interest using a modulated laser source. Given that the identified system must be accurate for all the swept frequencies, a heat flux waveform is looked for, with a Power Spectral Density comparable to that of a white noise. This calibration thus involves the realization of a specific experimental setup in laboratory that allows applying the heat flux on

the form of a random or Pseudo Random Binary Signal (PRBS) and measuring it precisely as well as the voltage drop at the thermocouple. This approach does not require knowing the thermophysical properties of materials as well as the exact location of the thermocouple. Also, the knowledge of the thermocouple inertia is circumvented since it is considered within the calibration. From a theoretical point of view, the identified system is the direct model when solving the inverse heat conduction problem. It means that the identified system and the voltage drop measurement at the sensor during the use of the sensor for a given application is sufficient to estimate the heat flux. This approach does not depend on a particular sensor geometry which then allows manufacturing also particular sensor geometries for applications. Major drawback of this approach is that the calibration must be realized in the same conditions than those encountered on the process during the use of the heat flux sensor otherwise a linear behaviour must be assumed. In other words, one must reproduce in the laboratory the same boundary conditions in terms of transient duration and magnitude of heat flux.

5.2 System identification hardware

The sensor consists of a cylindrical copper tube, where a thermocouple is integrated. The tip is of spherical form. The thermocouple is of type K with a junction diameter of 0.08 mm. As specified by the manufacturer, the rise time for the thermocouple is about 120 msec. However, nowadays the heat flux sensor must be used on comparable time duration, but with 0.1 msec sampling interval.

Figure 12 shows the schematic view of the “scale 1” experimental setup for these calibration measurements. Since the null-point calorimeter is used to measure very high heat flux densities up to 100 MW/m², the laser pulse energy must be high to achieve a sufficiently resolvable signal of the thermocouple. The laser in use is a laser diode that can provide 2000 W at 980 nm wavelength. It is known in system identification, that the best results are achieved when laser pulses of variable length are generated to better distinguish each of the characteristic times of the system: the diffusion in the tip, the response of the thermocouple and the influence of the interfaces. The laser is driven using a function generator that can generate a Pseudo Random Binary Signal (PRBS) for example. In Figure 13, the Power Spectral Density (PSD) of such a signal is compared to that of a Dirac function and that of the Heaviside function. It is obvious that the best representation of the frequencies is given by a perfect Dirac function which is very difficult to implement experimentally, particularly in terms of reproducibility. Concerning the two others, the best one is the PRBS because its PSD is superior to the Heaviside function PSD in the studied frequency range.

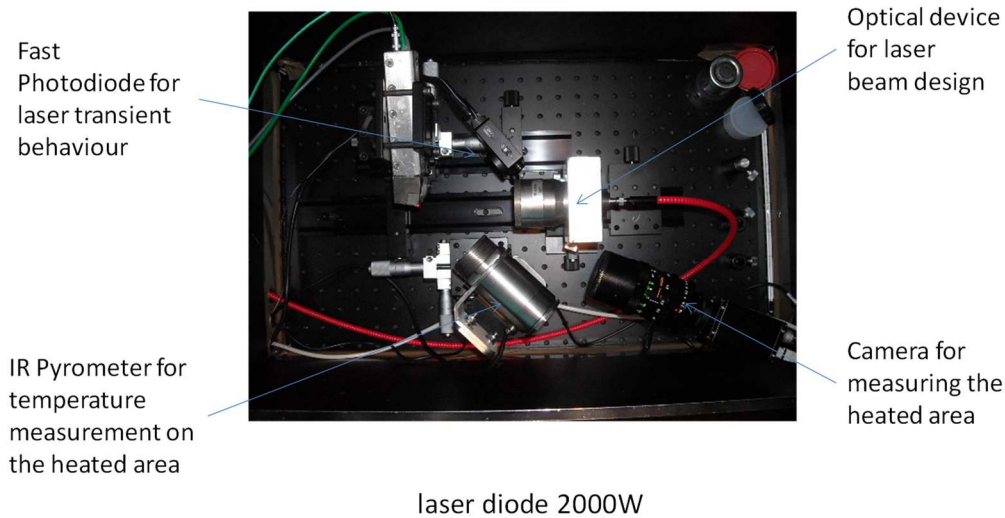


Figure 12: system identification hardware at scale 1

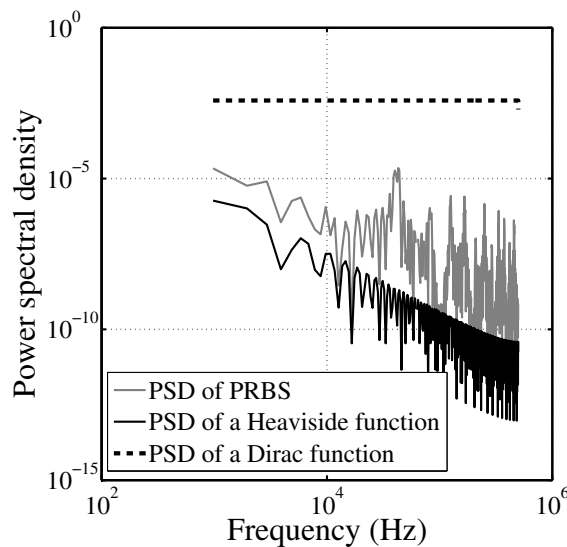


Figure 13: Power Spectral Density of a Dirac function, a Heaviside function and a PRBS.

A very small part (less than 2%) of the heat flux from the laser is recorded using a fast photodiode. All data are recorded using a fast oscilloscope. Moreover, the thermocouple data is amplified with a constant gain of 250. The incident heat flux density for the laser is deduced from the calibration curve of the manufacturer based on blackbody absorption. The sensor is made of copper which has been oxidized in a furnace at 400°C during four hours in order to

achieve high surface catalycity and to reach high absorptivity. Its emissivity has then been measured and is equal to 0.7 at the laser wavelength.

The measurement noise at the thermocouple is recorded without heating the sensor by the laser and results (sampling time is 100 μ sec) and the noise histogram presented in Figure 14 shows that the noise has a Gaussian distribution. On the other hand, the computation of the noise auto-correlation function is represented in Figure 15. This function is close to 0 from the second point and is thus equivalent to a Dirac function. In conclusion, all the assumptions concerning the measurement noise have been checked and the application of the least square algorithm to estimate the parameters of the non-integer system is fully consistent.

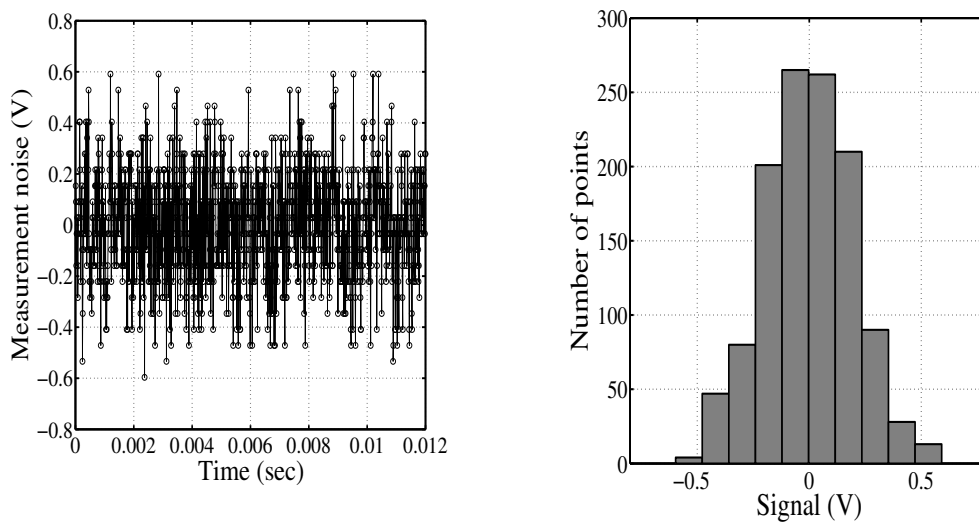


Figure 14: Noise measurement and noise distribution function.

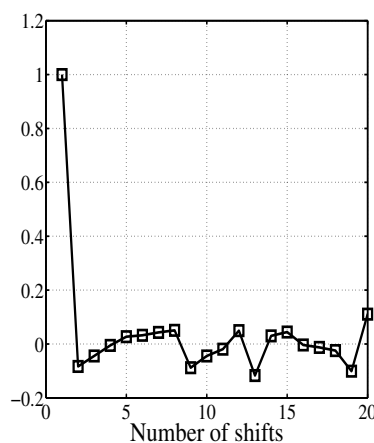


Figure 15: Autocorrelation function applied to the noise measurement.

The uncertainty for the measured emissivity is about 6%. Concerning the laser heat flux measured with a fan cooled broad band sensor, the constructor gives a calibration certificate and a relative precision of about 1%. Finally, the radius of the beam laser is measured manually, and the uncertainty is estimated to be 5%. In conclusion, the uncertainties of the measured heat flux density absorbed by the sensor is approximately 17% which is high compared to the uncertainties involved by the parameter estimation method.

For this tutorial an experimental setup at scale 1/400 has been realized. Indeed, the laser diode maximum power is 5W. It is driven through a National Instrument card under Labview software. The other parts of the experiment remain identical to those of the experiment at scale 1.

5.3 Heat transfer model in the fluxmeter

Thermal properties of the fin are λ for the thermal conductivity, α for the thermal diffusivity, ρ for the density and C_p for the specific heat. Heat losses between the fin and the surrounding fluid are characterized by a heat exchange coefficient h . The section of the thin is denoted S and the circumference is denoted s . If the temperature depends only on the longitudinal direction, (with a Biot number $Bi = h d/\lambda \ll 0.1$) carrying out a heat flux balance on a slice of the fin of width Δx , we get:

$$\phi_e - \phi_s - \phi_p = \rho C_p S \Delta x \frac{dT}{dt} \quad (74)$$

with:

$$\phi_e = -\lambda S \frac{dT(x,t)}{dx} \quad (75)$$

$$\phi_s = -\lambda S \frac{dT(x+\Delta x,t)}{dx} \quad (76)$$

$$\phi_p = h s \Delta x (T(x,t) - T_\infty) \quad (77)$$

Substituting these relations into (74) we obtain:

$$\lambda S \left(\frac{dT(x+\Delta x,t)}{dx} - \frac{dT(x,t)}{dx} \right) - h s \Delta x (T(x,t) - T_\infty) = \rho C_p S \Delta x \frac{dT(x,t)}{dt} \quad (78)$$

that is,

$$\lambda S \frac{d^2T(x,t)}{dx^2} \Delta x - h s \Delta x (T(x,t) - T_\infty) = \rho C_p S \Delta x \frac{dT(x,t)}{dt} \quad (79)$$

Putting $T'(x) = T(x) - T_\infty$, the above expression becomes:

$$\lambda S \frac{d^2T'(x,t)}{dx^2} - h s T'(x,t) = \rho C_p S \frac{dT'(x,t)}{dt} \quad (80)$$

Applying the Laplace transform to T' , we obtain:

$$\frac{d^2\theta(x,p)}{dx^2} - k^2\theta(x,p) = 0 \quad (81)$$

with

$$k^2 = \frac{\rho C_p S p + h s}{\lambda S} = \frac{p}{\alpha} + \frac{h s}{\lambda S} \quad (82)$$

The solution is:

$$\theta(x, p) = A \exp(k x) + B \exp(-k x) \quad (83)$$

When $x \rightarrow \infty$ we find $A=0$. Then:

$$\theta_0 = L(T(0, t) - T_\infty) = B \quad (84)$$

and thus:

$$\theta(x, p) = \theta_0 \exp(-k x) \quad (85)$$

The heat dissipated by the semi-infinite fin is:

$$\psi_0(p) = -\lambda S \left. \frac{d\theta(x, p)}{dx} \right|_{x=0} \quad (86)$$

that is,

$$\theta(x, p) = \frac{\psi_0(p)}{\lambda S k} \quad (87)$$

Relation (87) shows that thermal impedance of the fin is:

$$Z_a = \frac{\exp(-k x)}{\lambda S k}, k = \sqrt{\frac{p}{\alpha} + \frac{h s}{\lambda S}} \quad (88)$$

5.4 Correlation and spectral techniques

During the tutorial we will generate 2 kinds of heat flux sequence.

5.4.1 Linear swept-frequency cosine signal

We will consider first a heat flux of the form of a linear swept-frequency cosine signal:

$$\varphi_0(t) = \sin(2\pi f(t)t) \quad (89)$$

The frequency varies linearly with time as:

$$f(t) = f_0 + \frac{f_1 - f_0}{t_1} t, 0 \leq t \leq t_1 \quad (90)$$

f_0 is the instantaneous frequency at time 0, and f_1 is the instantaneous frequency at time t_1 (see Figure 16).

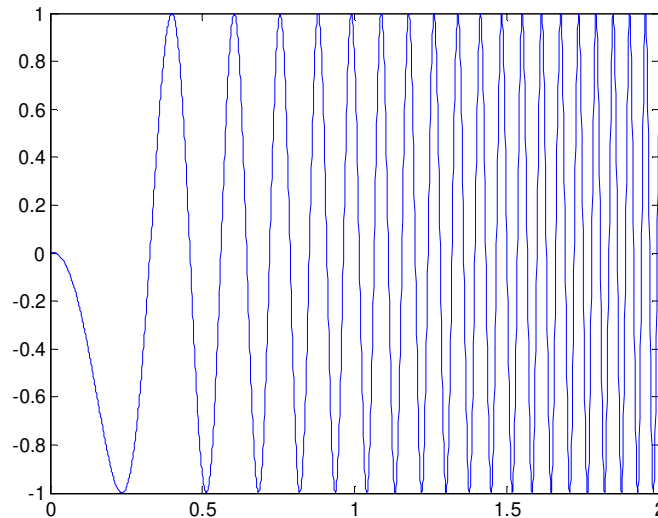


Figure 16: example of linear swept-frequency cosine signal with $f_0 = 0.1\text{Hz}$ and $f_1 = 10\text{Hz}$.

The Welch technique will be used here. The swept-frequency cosine heat flux waveform has two major interesting features. The first is that the offset must be easily removed from the experimental heat flux in order to fully satisfy the relation. The second feature is that the explored frequential domain, defined from the sensitivity analysis, is perfectly swept. Furthermore, the use of auto and cross power spectral density functions allows defining the so called coherence function as:

$$C_{y_0\varphi}(f) = \frac{|S_{y_0\varphi}(f)|^2}{S_{y_0y_0}(f)S_{\varphi\varphi}(f)} \quad (91)$$

This function can be viewed as the correlation coefficient between the temperature and the heat flux and lies between 0 and 1. If it is 1 at a certain frequency, then there is perfect correlation between the two signals at this frequency. In other words, there is consequently no noise interfering at this frequency, which leads to:

$$S_{\varphi e}(f) = S_{y_0y_0}(f)(1 - C_{y_0\varphi}(f)) \quad (92)$$

5.4.2 PRBS signal

In a second stage we will consider the heat flux sequence as a Pseudo Random Binary Signal (PRBS). “White noise” is the term given to completely random unpredictable noise, such as the hiss you hear on an untuned radio. It has the property of having components at every frequency. A pseudo-random binary sequence (PRBS) can also have this property but is entirely predictable. A PRBS is rather like a long recurring decimal number- it looks random if you examine a short piece of the sequence, but it repeats itself every m bit. Of course, the larger m

is, the more random it looks. You can generate a PRBS with a shift register and an XOR gate. Connecting the outputs of two stages of the shift register to the XOR gate, and then feeding the result back into the input of the shift register will generate a PRBS of some sort. Some combinations of outputs produce longer PRBSs than others- the longest ones are called m-sequences (where m means “maximum length”). A binary sequence (BS) is a sequence of N bits,

$$a_j \text{ for } j = 0, 1, \dots, N - 1,$$

i.e. m ones and $N - m$ zeros. A BS is pseudo-random (PRBS) if its autocorrelation function:

$$C(v) = \sum_{j=0}^{N-1} a_j a_{j+v} \quad (93)$$

has only two values:

$$C(v) = \begin{cases} m, & \text{if } v \equiv 0 \pmod{N} \\ m \times c, & \text{otherwise} \end{cases} \quad (94)$$

where

$$c = \frac{m-1}{N-1} \quad (95)$$

is called the duty cycle of the PRBS.

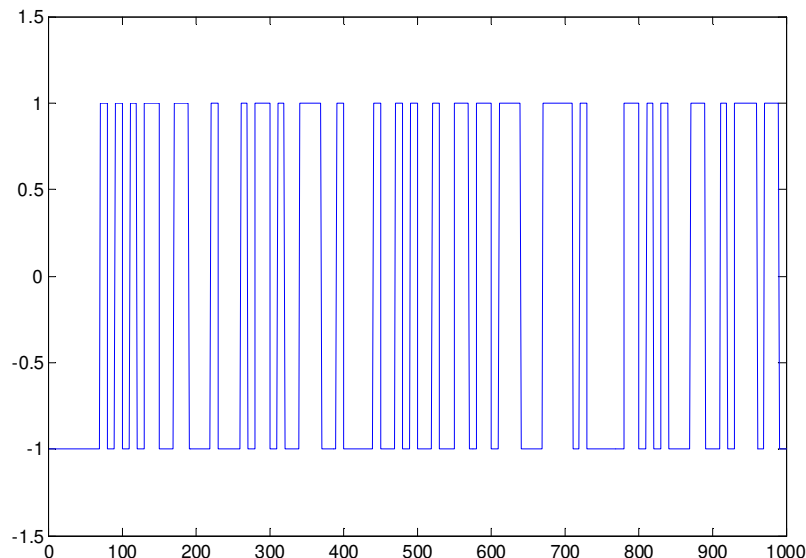


Figure 17: example of a PRBS sequence (X axis is the number of samples).

A PRBS is random in a sense that the value of an a_j element is independent of the values of any of the other elements, similar to real random sequences.

It is 'pseudo' because it is deterministic and after N elements it starts to repeat itself, unlike real random sequences, such as sequences generated by radioactive decay or by white noise. The PRBS is more general than the n -sequence, which is a special pseudo-random binary sequence of n bits generated as the output of a linear shift register. An n -sequence always has a 1/2 duty cycle and its number of elements $N = 2^k - 1$.

5.5 Parametric identification - AR models, theoretical background

As expressed by relation (88) heat transfer in a fin is modelled as:

$$\theta(x, p) = \frac{\exp(-k x)}{\lambda S k} \psi(p), \text{ with } k = \sqrt{\frac{p}{\alpha} + \frac{h s}{\lambda S}} \quad (96)$$

On the one hand, we can write:

$$k = \sqrt{\frac{p}{\alpha} + \frac{h s}{\lambda S}} = \sqrt{\frac{h s}{\lambda S}} \sqrt{\frac{\lambda S}{\alpha h s} p + 1} \quad (97)$$

Using the series expansion yields:

$$k = \sqrt{\frac{h s}{\lambda S}} \sqrt{\frac{\lambda S}{\alpha h s} p + 1} = \sqrt{\frac{h s}{\lambda S}} \sum_{n=0}^{\infty} \frac{(2n-1)!}{(2n)!} \left[\frac{1}{2} \frac{\lambda S}{\alpha h s} p \right]^n \quad (98)$$

On the other hand one has:

$$e^z = \sum_{n=0}^{\infty} \frac{z^n}{n!}, \quad \forall z \quad (99)$$

Replacing k in the exponential function and this exponential by its series, an equivalent expression of for relation (96) is obtained with the following form:

$$\sum_{n=0}^{\infty} \alpha_n s^{n+1} \theta_m(s) = \sum_{n=0}^{\infty} \beta_n s^n \Phi(s) \quad (100)$$

where α_n and β_n have complex but analytical expressions.

Considering the initial condition (temperature is zero at each point of the domain) and using the property:

$$L\left(\frac{d^n f(t)}{dt^n}\right) = s^n F(s) - \sum_{k=0}^{n-1} s^{n-k-1} \frac{d^k f(0)}{dt^k} \quad (101)$$

one shows that relation (100) is equivalent to:

$$\sum_{n=0}^{\infty} \alpha_n \frac{d^{n+1} T(M, t)}{dt} = \sum_{n=0}^{\infty} \beta_n \frac{d^n \varphi(t)}{dt} \quad (102)$$

Using the discrete form of the derivatives, an equivalent form of relation (102) is obtained, where temperature at time $k \Delta t$ is a function of the heat flux and of the temperature at previous times as:

$$T_k = b_0 \varphi_{k-nk} + b_1 \varphi_{k-nk-1} + \dots + b_{nb} \varphi_{k-nk-nb} - a_1 T_{k-1} - \dots - a_{na} T_{k-na}, \quad k = (1, \dots, N) \quad (103)$$

The method will be applied during the tutorial starting from the response to a PRBS sequence for the heat flux.

5.6 NI models, theoretical background

At very short times, heat losses are negligible with respect to the heat diffusion in the fin. Therefore:

$$\frac{p}{\alpha} \approx \frac{hs}{\lambda S} \text{ and } k \approx \sqrt{\frac{p}{\alpha}} \quad (104)$$

since:

$$\theta(x, p) = \sum_{n=0}^{\infty} \frac{(-kx)^n}{n!} \frac{1}{\lambda S k} \psi(p), \text{ with } k = \sqrt{\frac{p}{\alpha} + \frac{hs}{\lambda S}} \quad (105)$$

Replacing k in this relation leads to:

$$\theta(x, p) = \frac{\sum_{n=0}^{\infty} \frac{-x^n}{\alpha^{n/2} n!} p^{n/2}}{\sqrt{\lambda \rho C_p S} p^{1/2}} \psi(p) \quad (106)$$

That can be also written as:

$$\sqrt{\lambda \rho C_p S} p^{1/2} \theta(x, p) = \sum_{n=0}^{\infty} \frac{-x^n}{\alpha^{n/2} n!} p^{n/2} \psi(p) \quad (107)$$

We have shown in equation (56):

$$L\left(\frac{d^\nu f(t)}{dt^\nu}\right) = s^\nu F(s) - \sum_{k=0}^{n-1} s^{n-k-1} \frac{d^k f(0)}{dt^k} \quad (108)$$

This equation remains true even if ν is a real number or more generally complex. So we can express relation (107) in the time domain as:

$$\alpha_0 D^{n/2} \{T_m(t)\} = \sum_{n=0}^{\infty} \beta_n D^{n/2} \{\varphi(t)\} \quad (109)$$

with:

$$\alpha_0 = \sqrt{\lambda \rho C_p S} \text{ and } \beta_n = \frac{-x^n}{\alpha^{n/2} n!} \quad (110)$$

It appears thus that model (102) will not be accurate enough to describe the transient behaviour at the short times. As said in section 4 above, an optimal structure of a low order model for heat transfer problem by diffusion must be of the following form:

$$\sum_{n=0}^{\infty} \alpha_n D^{n/2} \{T_m(t)\} = \sum_{n=0}^{\infty} \beta_n D^{n/2} \{\varphi(t)\} \quad (111)$$

6 Conclusion

System identification is a powerful tool that allows the user to obtain a direct model to solve an inverse problem. In fact, this approach consists in applying a known thermal excitation and to measure the temperature at the sensors to find a relationship between these two quantities. Obviously, this approach finds an interest if the system is not well characterized in terms of its thermal properties (thermal conductivity, specific heat, density, heat exchange coefficient at the boundaries, thermal resistance at the interfaces). Moreover, this technique does not require knowing the exact locations of the sensors in the system as well as their dynamical behaviour. It means that a calibration of the sensors is not required since they are used both for the system identification and the inversion. The constraints encountered with such an approach are that the system must be identified in the same configuration in which it will be used during the inversion. It means first that the time range for the system identification will define the usable time domain for the direct model. On the other hand, all the boundary conditions experienced during the system identification must remain identical during the inversion.

Finally, it must be emphasized that the computational times for the inversion will be decreased very significantly even if the thermal system is complex. It is a very interesting feature of this approach since the simulation of the identified system is faster than that based on a discretization of the heat equation.

7 References

- [1] Ljung, L., *System identification. Theory for the user*, Prentice – Hall, inc., Englewood Cliffs, New Jersey, 1986.
- [2] Walter, E., Pronzato, L., *Identification de modèles paramétriques à partir de données expérimentales*, Collection Modélisation Analyse Simulation et Commande, Éditions Masson, 1994.
- [3] Kay S.M., *Modern Spectral Estimation*, Englewood Cliffs, NJ: Prentice-Hall, 1988.
- [4] Stoïca P. and Moses R., *Introduction to spectral analysis*, Upper Saddle River, NJ: Prentice-Hall, 1997.
- [5] Welch, P. D., *The use of Fast Fourier Transform for the estimation of power spectra: a method based on time averaging over short, modified periodograms*, IEEE Trans. Audio Electroacoust., Vol. AU-15, 70-73, June 1967.
- [6] Battaglia J.-L., Batsale J.-C., *Estimation of heat flux and temperature in a tool during turning*, Inverse Problems in Engineering, vol. 8, p.435-456,2000.
- [7] Battaglia J.-L., Le Lay L., Batsale J.-Ch. L., Oustaloup A., Cois O., *Utilisation de modèles d'identification non entiers pour la résolution de problèmes inverses en conduction*, International Journal of Thermal Science, Vol. 39, pp. 374-389, 2000.
- [8] Battaglia J.-L., Cois O., Puigsegur L., Oustaloup A., *Solving an inverse heat conduction*

- problem using a non-integer identified model*, Int. J. Heat Mass Trans., 44, 2001, pp. 2671-2680.
- [9] Beck J., Blackwell B., St. Clair C.R., *Inverse Heat Conduction*, A Wiley-Interscience Publication, 1985.
- [10] Maillet D., André S., Batsale J.-C., Degiovanni A. et Moyne C., *Thermal quadrupoles. Solving the heat equation through integral transforms*, ed. Wiley, 2000.
- [11] Fourier J., *Théorie analytique de la chaleur*, Paris, 1822.
- [12] Liouville J., *Mémoire sur quelques questions de géométrie et de mécanique, et sur un nouveau genre pour répondre ces questions*, Jour.Ecole Polytech. 13 (1832) 1-69.
- [13] Oldham K. B., Spanier J., *The fractional calculus*, Academic Press, New York and London, 1974.
- [14] Oldham K. B., Spanier J., *The replacement of Fick's laws by a formulation involving semi differentiation*, Electroanalytical Chemistry and Interfacial Electrochemistry 26 (1970) 331-341.
- [15] Oldham K. B., Spanier J., *A general solution of the diffusive equation for semi-infinite geometries*, Journal of Mathematical Analysis and Applications 39 (1972) 655-669.
- [16] Battaglia J.-L., Le Lay L., Batsale J.-C., Oustaloup A., Cois O., *Heat flow estimation through inverted non integer identification models*, International Journal of Thermal Science 39 (3) (2000) 374-389.
- [17] Battaglia J.-L., Cois O., Puigsegur L., Oustaloup A., *Solving an inverse heat conduction problem using a non-integer identified model*, Int. J. of Heat and Mass Transfer 14 (44) (2000) 2671-2680.

8 Appendix 1: Matlab codes

We denote $z=[y \ u]$, the experimental data, where u is the input (heat flux) and y is the output (the temperature of the sensor)

8.1 Correlation method

```
function ir=correlation(z,M)
%   ir: the estimated impulse response
%   M: The number of lags for which the functions are computed

Rft = covar(z,M+1);
r(:,1) = (-M:1:M)';
r(M+1:2*M+1,2:3) = Rft([1 4],:)' ;
r(1:M,2:3) = Rft([1 4],M+1:-1:2)';
scir = Rft(4,1); sccf = sqrt(Rft(1,1)*Rft(4,1));
r(M+1:2*M+1,4) = Rft(2,:)' /sccf;
r(1:M,4) = Rft(3,M+1:-1:2)' /sccf;
ir = r(M+1:2*M+1,4)*sccf/scir;

function R=covar(z,M)
% Computes the covariance for z
```



```
% M: The maximum delay - 1, for which the covariance function is
estimated.
```

```
[Nft,nz]=size(z);
nfft = 2.^ceil(log(2*Nft)/log(2));
Yft=fft([z(:,1)' zeros(1,Nft)]),nfft);
Uft=fft([z(:,2)' zeros(1,Nft)]),nfft);
YUft=Yft.*conj(Uft);
UAft=abs(Uft).^2;
YAft=abs(Yft).^2;
RYft=fft(YAft,nfft);
n=length(RYft);
sumnft = sumnft+Nft;
R=real(RYft(1:M))/n;
```

8.2 Spectral method

```
function H = TF(z,N,M)
```

```
% The transfer function H is estimated at N equally spaced frequencies
between 0 (excluded) and pi.
% A smoothing operation is performed on the raw spectral estimates using a
Hamming Window, giving a frequency resolution of about pi/M.
```

```
[Ncap,nz] = size(z);
M = M/2; % this is to make better agreement with SPA.
M1 = fix(1/M);sc=1/(2*N);

u = z(:,2);

y = z(:,1);

nfft = 2*ceil(Ncap/N)*N;
Yft = fft(y,nfft,1);
Uft = fft(u,nfft,1);
Yft = [Yft(1-M1+2:1,:);Yft];
Uft = [Uft(1-M1+2:1,:);Uft];
Yft = Yft.*conj(Uft);
Uft = abs(Uft).^2;
ha = .54 - .46*cos(2*pi*(0:M1)'/M1);
ha = ha/(norm(ha)^2);
Yft = filter(ha,1,Y);
Uft = filter(ha,1,U);
Yd = Yd+Yft(M1+fix(M1/2)+sc:sc:M1+fix(M1/2)+1/2,,:);
Ud = Ud+Uft(M1+fix(M1/2)+sc:sc:1/2+M1+fix(M1/2),,:);
H = Yd./Ud;
```

8.2.1 Parametric estimation

```
function [n_ord,num,d_ord,den,rsdi,ecn,ecd] =
ni_sid_ident_rec(u,y,time,num_def,den_def,adm,adg,teta0)
```

```

%
% Fonction ni_sid_ident_rec
%
% Identification of non integer model using recursive least square algorithm
%
% Input Argument
%
% u,y: system input and output
% time: time vector
% num_def: numerator (first line orders and second line 0 for unknown
% parameters else give the value)
% den_def: denominator (first line orders and second line 0 for unknown
% parameters else give the value)
% adm: Adaptation mechanism. adg: Adaptation gain
% adm='ff', adg=lam: Forgetting factor algorithm, with forg factor
lam
% adm='kf', adg=R1: The Kalman filter algorithm with R1 as covariance
% matrix of the parameter changes per time step
% adm='ng', adg=gam: A normalized gradient algorithm, with gain gam
% adm='ug', adg=gam: An Unnormalized gradient algorithm with gain gam
% teta0: initial value of the parameters
%
% Output Argument
%
% num,den: denominator and numerator coefficient
% n_ord, d_ord: order of the numerator and denominator
% rsdi: residuals
% ecn, ecn: standard deviation for the estimated parameters
%
% Jean-Luc Battaglia
%
adm=lower(adm(1:2));
if ~(adm=='ff'|adm=='kf'|adm=='ng'|adm=='ug')
    error('The argument ADM should be one of ''ff'', ''kf'', ''ng'', or
    ''ug''.')
end
if adm(2)=='g', grad=1;else grad=0;end
%
n_ord=num_def(1,:); d_ord=den_def(1,:); %
derivation order
d_ord_ukn=find(den_def(2,)==0); n_ord_ukn=find(num_def(2,)==0); %
orders associated to unknown parameters
d=length(d_ord_ukn)+length(n_ord_ukn); %
number of unknown parameters
d_ord_knw=find(den_def(2,)!=0); n_ord_knw=find(num_def(2,)!=0); %
orders associated to unknown parameters
%
p=10000*eye(d);
if nargin < 8, teta=eps*ones(d,1); else teta=teta0; end
if adm(1)=='f', R1=zeros(d,d); lam=adg;end;
if adm(1)=='k', [sR1,SR1]=size(adg);
    if sR1~=d | SR1~=d
        error(['The R1 matrix should be a square matrix with dimension
',...
                'equal to number of parameters.'])
    end
end

```

```

end;
R1=adg; lam=1;
end;
%
Yf=dn(time(2)-time(1),y,d_ord); Uf=dn(time(2)-time(1),u,n_ord); % matrice
de régression complète (pour tous les ordres)
%
phi=[-Yf(:,d_ord_ukn) Uf(:,n_ord_ukn)]; % regression vector
%
yn=[Yf(:,d_ord_knw) -Uf(:,n_ord_knw)]*[den_def(2,d_ord_knw)
num_def(2,n_ord_knw)]';
%
rsdi=0;
for kcou = 1:length(u)-1,
    yh=phi(kcou,:)*teta; % ym(t+1)
    if ~grad,K=p*phi(kcou,:)/(lam + phi(kcou,:)*p*phi(kcou,:)); % k(t+1)
        p=(p-K*phi(kcou,:)*p)/lam+R1; % p(t+1)
    else K=adg*phi(kcou,:);end;
    if adm(1)=='n', K=K/(eps+phi(kcou,:)*phi(kcou,:));end;
    epsi=yn(kcou)-yh; % y(t+1)-ym(T+1)
    rsdi=rsdi+epsi^2;
    teta=teta+K*epsi; % pmc(t+1)=pmc(t)+k(t+1)*(y(t+1)-ym(T+1))
end;
rsdi=sqrt(rsdi/kcou);
ec_teta=(rsdi/2).*sqrt(diag(p));
%
% Transfert function parameter computation from teta vector
den(d_ord_knw)=den_def(2,d_ord_knw);
den(d_ord_ukn)=teta(1:length(d_ord_ukn));
ecd(d_ord_knw)=0;ecd(d_ord_ukn)=ec_teta(1:length(d_ord_ukn));
num(n_ord_knw)=num_def(2,n_ord_knw);
num(n_ord_ukn)=teta(length(d_ord_ukn)+1:end);
ecn(n_ord_knw)=0;ecn(n_ord_ukn)=ec_teta(length(d_ord_ukn)+1:end);

function [dy,Erreur]=dn(time,x,n)

% [dy,Erreur]=dn(time,x,n)
%
% This function computes the derivate of order n, with n complex vector,
% of the data x ; time is the sampling period or the time vector
%
% Argument in :
% time : vector time of the vector x (scalar vector) or sample (scalar)
% x : data (complex matrix)
% n : order of the derivate (complex vector)
%
% Argument out :
% dy : data (complex matrix)
%
%
S_time=size(time);
S_x=size(x);
S_n=size(n);

```

```
%sampling time interval
h=[time(2);time(2:end)]-[time(1);time(1:end-1)];
Ak=binome(n,S_x(1));
A=Ak;

%derivative computation
dy=zeros(S_x(1),S_x(2));
y=zeros(S_x(1),1);

for col=1:S_x(2)
    y=conv(x(:,col),A(:,col));
    dy(:,col)=y(1:S_x(1))./h.^n(1,col);
end;
```

9 Appendix 2: the non-integer calculus

Let us consider $f(t)$ an integrable function integrable, definite and bounded, on (a, ∞) upon which we make n successive integrations. One obtains:

$${}_a I_t^n f(t) = \int_a^t du_1 \int_a^{u_1} du_2 \cdots \int_a^{u_{n-1}} f(u_n) du_n = \frac{1}{(n-1)!} \int_a^t (t-u)^{n-1} f(u) du \quad (1)$$

Since $(n-1)! = \Gamma(n)$, it is easier to generalize the previous relation to any number n real, and more generally complex, and then to define the integral of real order ν ($\text{Re}\nu > 0$), or more simply the non-integer integral as:

$${}_a I_t^\nu f(t) = \frac{1}{\Gamma(\nu)} \int_a^t (t-u)^{\nu-1} f(u) du, \quad \text{Re}\nu > 0 \quad (2)$$

With $\Gamma(\nu)$ the Eulerian function of second specie defined by:

$$\Gamma(\nu) = \int_0^\infty u^{\nu-1} \exp(-u) du \quad (3)$$

The non-integer integral is like the convolution product between function $t^{\nu-1}$ and function $f(t)$. It is usual to restrain the lower bound of the integral to $a=0$, that corresponds to the initial time of the experiment. This leads to the definition of the non-integer integral of order ν in the sense of Reimann-Liouville and we note $I^\nu f(t) = {}_0 I_t^\nu f(t)$. The additive property upon the integration order is expressed as:

$$I^\nu I^\mu f(t) = I^{\nu+\mu} f(t), \quad \forall \text{Re}(\nu, \mu) > 0 \quad (4)$$

This leads to the non-integer derivative of order ν as:

$$D^\nu f(t) = D^n I^{n-\nu} f(t) \quad n \in \mathbb{N}, \text{Re}(\nu) > 0, \quad n-1 \leq \text{Re}(\nu) < n \quad (5)$$

From those definitions, it appears that the non-integer derivation of function $f(t)$ at time t is expressed according to the entire set of values of the function from the initial time until time t . This operator has therefore an infinite memory effect that distinguishes it fundamentally from the classical derivative of integer order. However, the values of the function previous to time t are weighted by a forgotten factor that is as high as one approaches the initial time.

The discrete representation of the non-integer derivative has been given by Grünwald and is expressed as:

$$D^\nu f(t) = \lim_{h \rightarrow 0} \frac{\Delta_h^\nu f(t)}{h^\nu}, \quad \nu > 0, \quad (6)$$

Δ_h^ν represents the non-integer increase defined by:

$$\Delta_h^\nu f(t) = \sum_{j=0}^N (-1)^j \binom{\nu}{j} f(t - jh), \quad t = Nh \quad (7)$$

With:

$$\binom{\nu}{j} = \frac{\nu(\nu-1)\cdots(\nu-j+1)}{j!} \quad (8)$$

Let us note that the sampling time interval h must be necessary constant with this definition.